0026-895X/97/030448-14$3.00/0

MOLECULAR PHARMACOLOGY, **51:**448–461 (1997).

Copper-Dependent Oxidative and Topoisomerase II-Mediated DNA Cleavage by a Netropsin/4′-(9-acridinylamino)methanesulfon-*m*-anisidide Combilexin

JEAN-PIERRE HENICHART, MICHAEL J. WARING, JEAN-FRANCOIS RIOU, WILLIAM A. DENNY, and CHRISTIAN BAILLY

Institut de Chimie Pharmaceutique, Université de Lille II, 59006 Lille, France (J.-P.H.), Department of Pharmacology, University of Cambridge, Cambridge CB2 1QJ, UK (M.J.W.), Rhône-Poulenc Rorer, Centre de Recherche de Vitry-Alfortville, 94403 Vitry sur Seine, France (J.-F.R.), Cancer Research Laboratory, University of Auckland School of Medicine, Auckland, New Zealand (W.A.D.), and Institut de Recherches sur le Cancer, Institut National de la Santé et de la Recherche Médicale Unité 124, 59045 Lille, France (C.B.)

Received July 2, 1996; Accepted October 20, 1996

SUMMARY

A conjugate molecule was synthesized by linking the DNA-intercalative antitumor drug 4′-(9-acridinylamino)methanesulfon-*m*-anisidide (mAMSA) via a 4-carboxamide side chain to a dipyrrolecarboxamide moiety structurally related to the minor groove-binding antibiotic netropsin. The molecule (netropsin/mAMSA) behaves as a threading intercalator. Its netropsin-like tail becomes located in the minor groove of the double helix and serves to drive the hybrid molecule preferentially to AT-rich sites on various DNA fragments as revealed by DNase I footprinting. The hybrid retains the susceptibility to copper-dependent oxidation characteristic of the parent mAMSA moiety as well as its ability to generate oxygen radicals, which can mediate DNA damage, mainly at cytidine and guanosine nucleotides. It also retains the property of stimulating the formation of cleavable complexes with DNA in the presence of topoisomerase II, but its netropsin-like moiety confers little or no influence on the reaction with topoisomerase I. Although netropsin/mAMSA is less potent than mAMSA at producing cleavable complexes with topoisomerase II, it promotes the appearance of cleavage sites at much the same nucleotide sequences as does the parent compound. The dipyrrolecarboxamide tail is not silent, however, since it modifies the concentration-dependence of cleavable complex formation.

Several antitumor antibiotics that bind strongly to DNA are constructed to behave simultaneously as a minor groove binder and an intercalator. Such is the case with actinomycin and doxorubicin, which are used extensively in the treatment of leukemias and solid tumors. Actinomycin possesses an intercalating phenoxazone chromophore substituted with two cyclic peptides that fit neatly into the minor groove of the double helix (1). Doxorubicin has a minor groove binding amino sugar residue attached to the intercalating anthracycline moiety (2). In both cases, the two functional parts of each drug molecule are involved in the recognition of particular DNA sequences (3, 4). Similar binding characteristics have been reported with other potent cytotoxins, such as echinomycin and neocarzinostatin (5, 6). A few years ago, these observations prompted us to develop intercalator-minor groove binder hybrid molecules that are now usually referred to as combilexins (7). Different series of combilexin molecules, containing an oligopyrrolecarboxamide moiety attached to a polycyclic aromatic ring (e.g., acridine, ellipticine, flavin, porphyrin, anthraquinone), have been synthesized, and their DNA-binding and biochemical properties have been investigated. The potential of these hybrid molecules is wide ranging and includes (i) enhanced DNA-binding strength and selectivity, (ii) interference with topoisomerases, and (iii) facilitation of the cellular transport of the drugs, promoting their potential use in cancer chemotherapy.

We report on a second-generation combilexin that consists of a minor groove-binding moiety structurally related to netropsin linked to the antitumor drug mAMSA, which is an anilino-aminoacridine derivative that is used for the treatment of acute myelogenous leukemia (8). It is commonly assumed that the antitumor activity of mAMSA arises primarily from its capacity to intercalate into DNA, thus inhib-

This work was supported by research grants from Institut National de la Santé et de la Recherche Médicale (C.B.), Ligue Nationale Contre le Cancer (Comité du Nord) (C.B.), Association pour la Recherche sur le Cancer (C.B.), Cancer Research Campaign (M.J.W.), Wellcome Trust (M.J.W.), Association for International Cancer Research (M.J.W.), and Sir Halley Stewart Trust (M.J.W.).

ABBREVIATIONS: mAMSA, 4′-(9-acridinylamino)methanesulfon-*m*-anisidide (amsacrine); bp, base-pair; SDS, sodium dodecyl sulfate; NetAmsa, netropsin-4′-(9-acridinylamino)methanesulfon-manisidide; MPE, methidiumpropyl-EDTA; mAQDI, $N^{1\prime}$-methanesulfonyl-$N^{4\prime}$-(9-acridinyl)-3′-methoxy-2′,5′-cyclohexadiene-1′,4′-diimine; mAQI, 3′-methoxy-4′-(9-acridinyl-amino)-2′,5′-cyclohexodiene-1′-one.

iting the activity of topoisomerase II leading to double-strand breaks in the DNA (9). As shown in Fig. 1, the Net/Amsa hybrid bears a positively charged terminal side chain, which is known to contribute significantly to the AT-selectivity of such ligands (10). In addition, unlike the netropsin-anilinoacridine derivatives previously studied (11), the new hybrid retains the *m*-methoxy and methanesulfonamide substituents on the anilino ring, which are considered to constitute key elements for the interference with topoisomerases and the maintenance of the redox properties of mAMSA. In terms of DNA recognition, the most important point is that the netropsin moiety is connected to the acridine ring via a 4-carboxamide side chain, whereas it was previously attached directly to the anilino group. The connector between the two DNA-binding units was modified to convert the drug from a classic intercalator to a threading intercalator, based on our earlier findings with mAMSA/4-carboxamide derivatives (12). Recently, we demonstrated that NetAmsa does thread through the DNA double helix so as to intercalate its acridine chromophore, leaving the netropsin moiety and the methanesulfonanilino group positioned within the minor and major grooves of the double helix, respectively (13). The hybrid molecule exhibits structural features reminiscent of the antitumor antibiotics nogalamycin (14) and pluramycin (15).

The metabolism of mAMSA involves rapid oxidation to the quinoneimine derivative mAQDI, which can react with amine or thiol compounds, such as glutathione, in cells (16). In aqueous solution, mAQDI can hydrolyze to the quinone imine mAQI, lacking the methanesulfonamido group; then, a further hydrolysis yields 9-aminoacridine (Fig. 2). It has been proposed that the metabolites of mAMSA may contribute to its cytotoxic activity because under some conditions, the two primary oxidation products (mAQDI and mAQI) are considerably more cytotoxic to L1210 cells *in vitro* than is mAMSA (17). The facile oxidation of mAMSA by molecular oxygen and copper can induce degradation of DNA via a multistep process, as depicted in Fig. 2. In the presence of Cu(I) and mAQDI, molecular oxygen is reduced to superoxide radical $O_2^{\cdot-}$, which can then rapidly dismute to give H_2O_2. The reaction of H_2O_2 with Fe(II) or Cu(I) (Fenton reaction) or with $O_2^{\cdot-}$ (Haber-Weiss reaction) leads to the production of the DNA-damaging hydroxyl radical $OH^{\cdot}$ (18, 19). Accordingly, the susceptibility of mAMSA to oxidation and its related capacity to promote DNA lesions in cells have led to the hypothesis that oxidative metabolism may contribute to the cytotoxicity of this drug. However, at least two lines of evidence contradict this hypothesis. First, oxygen is not required for toxicity in cultured cells (20). Second, there is a direct correlation between the formation of DNA/topoisomerase II cleavable complexes and the cytotoxicity of mAMSA and its derivatives (21). In fact, both topoisomerase II inhibition and oxidative activation could possibly contribute to the pharmacological activity because it has been shown that metabolic activation of mAMSA increases the production of drug-dependent topoisomerase-associated DNA lesions (22).

These considerations prompted us to investigate the effects of the netropsin/mAMSA combilexin NetAmsa on the catalytic activity of topoisomerase II *in vitro* and its kinetics of

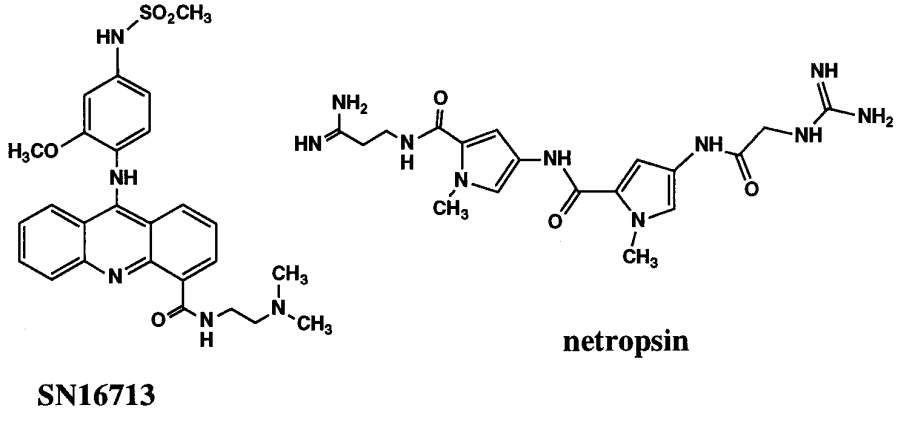

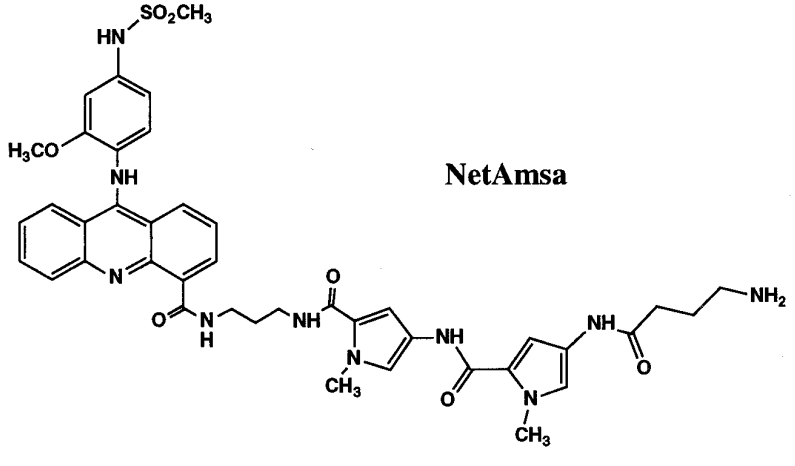

Fig. 1. Structures of netropsin, the mAMSA/4-carboxamide SN 16713, and the netropsin/mAMSA hybrid combilexin NetAmsa.

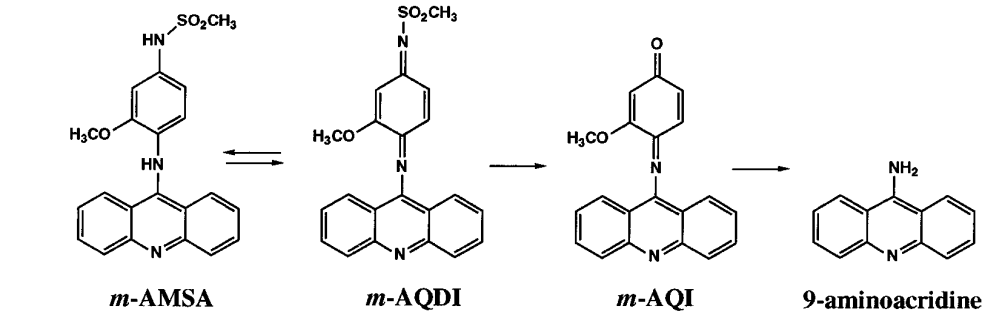

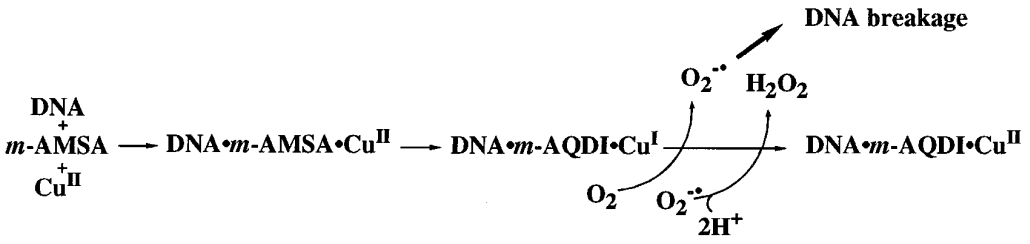

Fig. 2. *Top*, Oxidation of mAMSA by Cu(II) to mADDI and hydrolysis of mAQDI to mAQI which decomposes to 9-aminoacridine. *Bottom*, Proposed model for the degradation of DNA by mAMSA. A redox reaction of mAMSA and Cu(II) in the DNA-mAMSA-Cu(II) ternary complex leads to the formation of a DNA-mAQDI-Cu(I) complex which acts as a catalyst for Cu(I) to Cu(II) oxidation. The oxidation generates oxygen free radicals responsible for DNA breakage.

oxidation in the presence of copper ions. DNA sequencing methodology was used to determine whether the capacity of the conjugate to bind preferentially to AT-rich sequences correlates with the induced copper-dependent and/or topoisomerase II-mediated cleavage of DNA. The effects of the combilexin molecule were compared with those produced by mAMSA and the mAMSA/4-carboxamide derivative SN 16713 (Fig. 1), which is also a DNA-threading intercalator (23).

Materials and Methods

Drugs and Chemicals

Netropsin was purchased from Serva (Heidelberg, Germany). mAMSA, camptothecin, and MPE were from Sigma Chemical (La Verpillière, France). The synthesis of the mAMSA/4-carboxamide derivative SN 16713 has been reported (23). Drug concentrations were determined spectroscopically in 10-mm-pathlength quartz cuvettes using the following molar extinction coefficients: 21,500 M/cm at 296 nm for netropsin, 12,000 M/cm at 434 nm for mAMSA, 12,900 M/cm at 442 nm for SN 16713, and 13,000 M/cm at 440 nm for NetAmsa. All other chemicals were analytical-grade reagents.

Biochemicals

Plasmid DNA was isolated from *Escherichia coli* by a standard SDS-sodium hydroxide lysis procedure and purified by banding in CsCl-ethidium bromide gradients. The plasmid PBS was cut with *Eco*RI, treated with alkaline phosphatase, and then labeled at the 5′-end using T4 polynucleotide kinase (Pharmacia, Piscataway, NJ) and [γ-^{32}P]ATP (6000 Ci/mmol, New England Nuclear Research Products, Boston, MA). The linear labeled plasmid was further digested with *Pvu*II to generate the singly end-labeled DNA fragment, which was then purified by preparative nondenaturating polyacrylamide gel electrophoresis.

Synthesis of the NetAmsa Molecule

The strategy previously used for the synthesis of mAMSA/4-carboxamide derivatives was followed (23) (Fig. 3). Briefly, 9-oxoacridan-4-carboxylic acid (**1**) is treated with thionyl chloride to afford the corresponding acyl chloride (**2**), which is unstable and thus immediately reacts with the amine (**3**). The method for the preparation of mono-*tert*-butoxycarbonylalkanediamines such as compound **3** has been detailed previously (24). In anhydrous, mildly basic media at a low temperature, the aliphatic amine **3** reacts selectively with the acid chloride moiety of the dichloro compound **2**. The resulting 9-chloroacridine-4-carboxamide derivative (**4**) is then coupled with *N*-(4-amino-3-methoxyphenyl)methanesulfonamide (**5**) under mild conditions to furnish the *N*-*tert*-butyloxycarbonyl-protected mAMSA-4-carboxamide derivative (**6**). After deprotection under acid conditions, the functionalized mAMSA derivative (**7**) bearing the aminopropylcarboxamide side chain is condensed with the aminobutyramido-bispyrrole-carboxylic acid **8** mimicking the netropsin antibiotic via a conventional coupling procedure using dicyclohexylcarbodiimide and *N*-hydroxybenzotriazole. Alternatively, the condensation can be carried out via the agency of dicyclohexyl carbodiimide in the presence of a catalytic amount of 4-(dimethylamino)pyridine DMAP. Both methods are applicable and give approximately the same yields. The synthesis of the netropsin moiety (**8**) has been reported previously (25). Finally, deprotection of compound **9** under acid conditions and purification affords the mAMSA/4-carboxamide/netropsin hybrid molecule NetAmsa: m.p., 197–199°; IR (KBr) ν 3370–3310, 3200, 2965, 1680, 1655, 1535 cm^{-1}; high-resolution mass spectrometry 823.42586 (M + 1)$^+$; [^{1}H NMR (dimethylsulfoxide D6) δ 1.70 (m, 2 H, CH_2); 1.91 (m, 2 H, CH_2); 2.53 (m, 2 H, C_2CO); 2.90 (m, 2 H, CH_2NH_3^+); 3.12 (s, ^{3}H, SO_2CH_3); 3.40–3.50 (m, 4 H, CH_2NH); 3.55 (s, ^{3}H, OCH_3); 3.97 (2 s, 6 H, 2NC_3); 6.85–7.30 (m, 7 H, CH); 7.40–7.60 (m, ^{3}H, CH); 7.85–8.15 (m, 8 H, CH); 8.55 (m, 2 H, CH); 9.43 (s, 1 H, N); 9.81, 10.08, 10.27 (3 s, ^{3}H, NH); 11.52 (s, 1 H, NH); and 14.20 (s, 1 H, NH)].

Absorption Spectroscopy

Absorption spectra were recorded on a Uvikon-Kontron 810–820 spectrophotometer coupled to a Uvikon Recorder 21 and a Uvikon thermoprinter 48 (Paris, France). The cell holder (10 mm pathlength) was thermostated with a Haake unit. The absorbance between 300 and 600 nm was measured at time intervals of 4 or 10 min as indicated.

Chemiluminescence Measurements

Fresh solutions of lucigenin (bis-*N*-methylacridinium nitrate, Aldrich) were prepared before each experiment. Control samples contained 50 μM lucigenin in borate buffer. Samples were placed in an

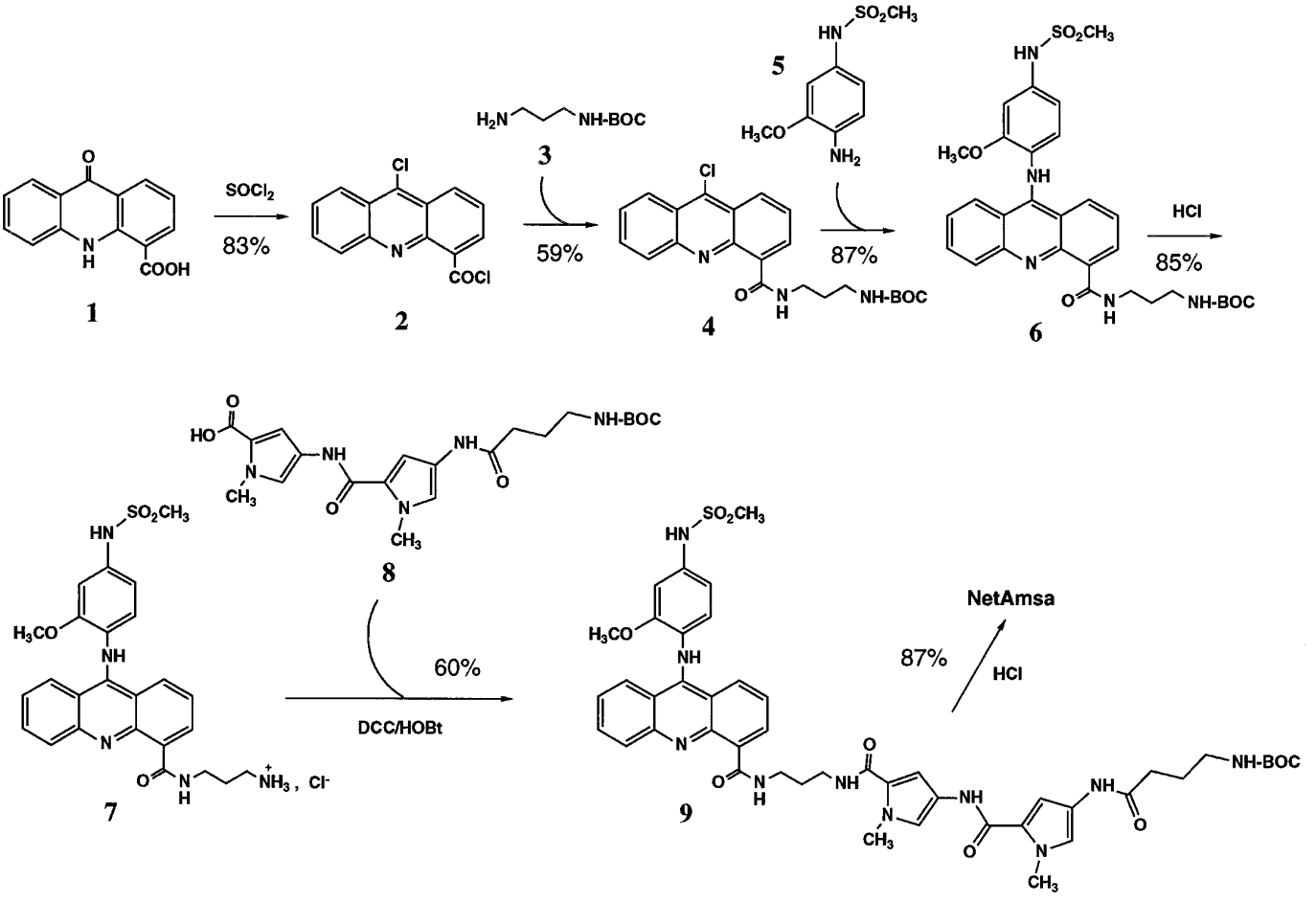

Fig. 3. Strategy used for the synthesis of mAMSA/4-carboxamide derivatives. *DCC*, dicyclohexylcarbodiimide; *HOBt*, N-hydroxybenzotriazole.

automated Packard (Meriden, CT) model 6500 Picolite luminometer, and the chemiluminescence response of each sample was measured by determining the total photon emission during a 30-sec counting period. Measurements were performed every 5 min for 1 hr. The pathway leading to lucigenin dioxygenation is shown in Fig. 4 (26).

The divalent reduction (with H_2O_2) and monovalent reduction (with $O_2^{\cdot-}$) of lucigenin lead to the formation of a dioxetane intermediate that disintegrates, yielding one excited-state and one ground-state molecule of *N*-methylacridone. The relaxation from the electronically excited state to the ground state is accompanied by an emission of light that is detected by the luminometer. The production of excited-state molecules and subsequent transfer of the molecular energy to light is directly dependent on the quantities of reactive oxygen species available to react with lucigenin.

Copper-Dependent Cleavage of DNA

Experiments with covalently closed circular DNA. Each reaction mixture contained 4 μl of supercoiled pBS DNA (3 μg), 5 μl of drug (2–300 μM), and 1 μl of $CuSO_4$. Reactions were performed in 50 mM sodium borate buffer, pH 9.4. After a ~16-hr (overnight) incubation at room temperature in the dark, 1 μl of loading buffer (0.25% bromphenol blue, 0.25% xylene cyanol, 30% glycerol in H_2O) was added to each tube, and the solution was loaded onto a 1% agarose gel. Electrophoresis was carried out for ~2 hr at 100 V in TBE buffer (89 mM Tris base, 89 mM boric acid, 2.5 mM Na_2-EDTA, pH 8.3). Gels were stained with ethidium bromide (1 μg/ml) and then destained for 30 min in water before being photographed under UV light.

Sequencing of copper-dependent DNA cleavage sites. Each reaction mixture contained 2 μl of ^{32}P-end-labeled DNA (117 mer or 265 mer from pBS), 6 μl of sodium borate buffer, pH 9.4, 10 μl of drug solution (2–300 μM), and 2 μl of 2 mM $CuSO_4$. Solutions of copper and drug were prepared fresh for each experiment. Samples (20 μl) were incubated overnight at room temperature in the dark and then lyophilized and washed twice with 50 μl of water before resuspension in 5 μl of an 80% formamide solution containing tracking dyes.

DNase I and MPE Footprinting

DNase I and MPE footprinting experiments were performed essentially according to the protocols recently described (27). Briefly, samples of the labeled DNA fragment were incubated with a buffered solution containing the desired drug concentration. After a 30–60-min incubation at 37° to ensure equilibration, the digestion was initiated by the addition of either the DNase I solution or (successively) MPE, $Fe(NH_4)_2(SO_4)_2{\cdot}6H_2O$ (freshly prepared), and dithiothreitol. In both cases, the extent of digestion was limited to <30% of the starting material to minimize the incidence of multiple cuts in any strand. After a 4-min incubation at room temperature, the reaction was stopped by freeze drying. Samples were lyophilized and washed at least twice with 50 μl of water. The DNA in each tube was resuspended in 5 μl of formamide-TBE loading buffer, denatured at 90° for 4 min, and then chilled in ice for 4 min before loading onto the sequencing gel.

Electrophoresis and Autoradiography

DNA cleavage products were resolved by electrophoresis under denaturing conditions in polyacrylamide gels (0.3 mm thick, 8% acrylamide containing 8 M urea). Electrophoresis was performed for ~2 hr at 60 W in TBE buffer. Gels were soaked in 10% acetic acid for 15 min, transferred to Whatman 3MM paper (Fairfield, NJ), dried

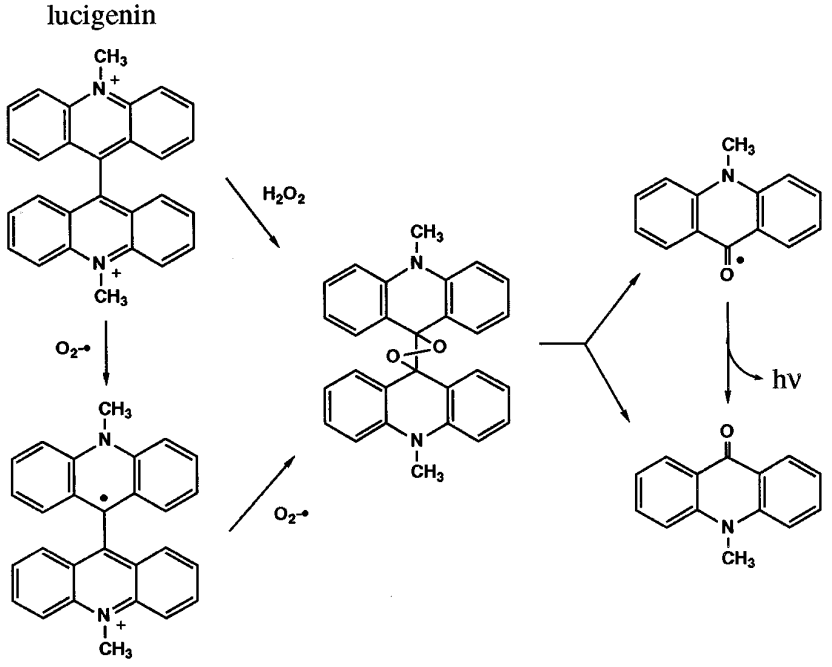

Fig. 4. Pathway leading to lucigenin dioxygenation (26).

under vacuum at 80°, and then analyzed with a Molecular Dynamics model 425E PhosphorImager (Sunnyvale, CA).

Quantification by Storage Phosphor Technology Autoradiography

Photostimulatable phosphor imaging plates (Kodak storage phosphor screens obtained from Molecular Dynamics) were pressed flat against dried sequencing gels and exposed overnight at room temperature. The PhosphorImager was used to collect all data. Baseline-corrected scans were analyzed by integrating all the densities between two selected boundaries using the ImageQuant version 3.3 software (Molecular Dynamics, Sunnyvale, CA). Each resolved band on the autoradiograph was assigned to a particular bond within the DNA fragment by comparison of its position relative to sequencing standards.

Topoisomerase I and II DNA Cleavage Reactions

Experiments with linear plasmid DNA on agarose gels. Topoisomerase I and topoisomerase II were purified from calf thymus. Human topoisomerase II (p170 form from TopoGEN, Columbus, OH) was also used. The cleavage reaction mixture contained 20 mM Tris·HCl, pH 7.4, 60 mM KCl, 0.5 mM EDTA, 0.5 mM dithiothreitol (plus 10 mM $MgCl_2$ and 1 mM ATP for topoisomerase II), 2×10^4 dpm of [α-^{32}P]pBR322 DNA, and the indicated drug concentrations. The reaction was initiated by the addition of topoisomerase I or II (20 units in 20 μl of reaction volume) and allowed to proceed for 10 min at 37°. Reactions were stopped by the addition of SDS to a final concentration of 0.25% and proteinase K to 250 μg/ml, followed by incubation for 30 min at 50°. For topoisomerase I, samples were denatured by the addition of 10 μl of denaturing loading buffer consisting of 0.45 M NaOH, 30 mM EDTA, 15% (w/v) sucrose, and 0.1% bromocresol green before loading onto a 1% agarose gel in TBE buffer containing 0.1% SDS. Electrophoresis was conducted at 2 V/cm for 18 hr.

Sequencing of topoisomerase II-mediated DNA cleavage sites. Each reaction mixture contained 2 μl of 5′-end ^{32}P-labeled DNA (117 mer or 265 mer from pBS), 4 μl of water, 2 μl of 10 × topoisomerase II buffer, and 10 μl of drug solution (2–300 μM). After a ≥30-min incubation to ensure equilibration, the reaction was initiated by the addition of 2 μl of purified topoisomerase II from calf thymus (as above) or human thymus (p170 form from TopoGEN). Samples were incubated for 40 min at 37° before the addition of SDS to 0.25% and proteinase K to 250 μg/ml to dissociate the drug/DNA/topoisomerase II cleavable complexes. The DNA was precipitated with ethanol, resuspended in 5 μl of formamide/TBE loading buffer, denatured at 90° for 4 min, and then chilled in ice for 4 min before loading onto the sequencing gel.

Effects of drugs on the formation and dissociation of DNA/topoisomerase II complexes. The 5′-end-labeled 265-bp fragment from plasmid pBS was incubated with mAMSA or NetAmsa at 10 μM for 45 min before addition of the enzyme. After reaction was allowed to occur for 1–60 min, complexes were dissociated by the addition of SDS/proteinase K and treated as described above. The reversibility experiments were performed as described previously (28). Briefly, preformed drug/DNA complexes were incubated with topoisomerase II for different periods of time (1–30 min) before the addition of a 50-fold excess of unlabeled DNA. Samples were treated with SDS/proteinase K.

Results

Copper-dependent oxidation. The oxidation of mAMSA to its quinoneimine metabolite mAQDI was induced *in vitro* by the addition of cupric ions Cu(II) ($CuSO_4$). The reaction can easily be monitored by UV spectroscopy because the absorption maxima of the oxidized and reduced species are well separated: the absorption spectrum of mAMSA exhibits two adjacent peaks at 432 and 414 nm, whereas the spectrum of mAQDI is characterized by two peaks at 374 and 355 nm (Fig. 5). We have taken advantage of these UV spectral characteristics to compare the kinetics of oxidation of the hybrid NetAmsa with those of its parent compounds mAMSA and SN 16713. Typical progress curves for the oxidation of the drugs in borate buffer, pH 9.4, are shown in Fig. 5. In each case, the addition of copper ions results in a decrease of the absorption at 450 nm and a simultaneous increase at 380 nm. The appearance of isosbestic points indicates that each drug is converted into a unique oxidized product. It can clearly be seen that the spectral changes are much more rapid with NetAmsa than with SN 16713. The rates of oxi-

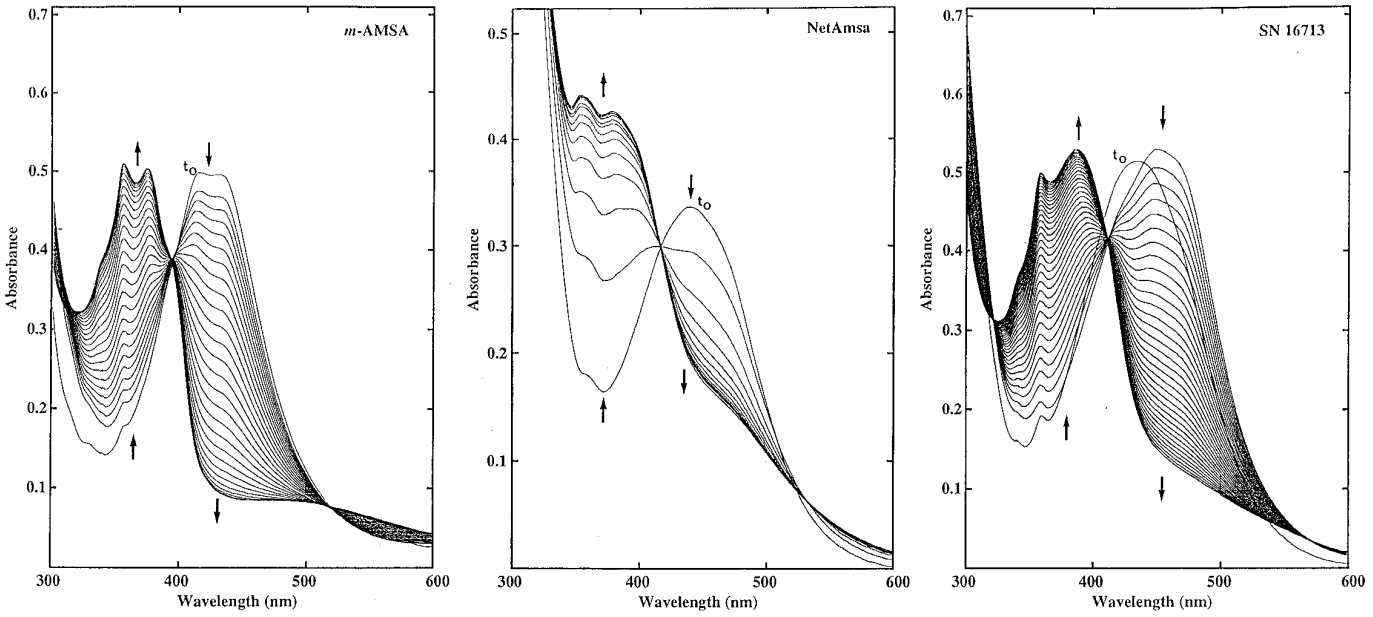

Fig. 5. Autoxidation of the drugs in the presence of copper. *Left*, 50 μM mAMSA and 150 μM $CuSO_4$. *Middle*, 50 μM NetAmsa and 50 μM $CuSO_4$. *Right*, 50 μM SN 16713 and 50 μM $CuSO_4$. Absorption spectra were recorded at intervals of 10 min for mAMSA and 4 min for NetAmsa and SN 16713. t_0, initial spectrum of each ligand before the addition of copper. *Arrows*, direction of change of the absorbance.

dation of the drugs can be compared directly by measuring the time necessary for half ($t_{1/2}$) and, less precisely but perhaps more usefully, for effectively complete (t) oxidation. The conversion of the anilino-amino group into a quinone imine group was considered to be complete when no further spectral changes could be detected. Experiments were performed at pH 9.4 (borate buffer) or pH 7.0 (Tris·HCl buffer) and with different drug/copper ratios. The data in Table 1 reveal that the reaction is more rapid with SN 16713 than with mAMSA and proceeds even faster with NetAmsa. For example, the time necessary for complete oxidation of the latter at pH 9.4 in the presence of an equimolar concentration of Cu(II) is approximately one third and one tenth of that required for oxidation of SN 16713 and mAMSA, respectively. It is interesting to observe that a slow but eventually complete oxidation of the drugs also takes place in the presence of 0.1 equivalent of copper, indicating that Cu(II) acts as a catalyst. At neutral pH, the oxidation reaction is much slower but the same kinetic order is observed: NetAmsa > SN 16713 > mAMSA. Therefore, we conclude that the introduction of a carboxamide side chain at position 4 of the acridine ring potentiates the oxidation process, presumably by raising the redox potential. In addition, the linkage of the netropsin moiety to the carboxamide side chain further activates the conversion of NetAmsa into the quinoneimine form because it oxidizes more rapidly than SN 16713. The newly introduced side chain must stabilize the drug/copper complex. Indeed, an ESR spectrum of a Cu(II)/NetAmsa mixture was obtained from a frozen aqueous solution (0.5 mM) in the presence of $CuSO_4$ (0.1 mM) at 77° K and 9.32 GHz (data not shown). The magnetic parameters are $A_{//}$ = 190 G, $g_{//}$ = 2.20, and $g_{\perp}$ = 2.03, suggesting that the copper is tetracoordinated. Such an ESR spectrum could also be obtained with SN 16713 but not with mAMSA.

TABLE 1
Kinetic parameters of oxidation

	Cu/drug ratio	$t_{1/2}$	t
		min	
pH 9.4			
mAMSA	0.1		
SN 16713	0.1	95	300
NetAmsa	0.1	45	180
mAMSA	1	135	345
SN 16713	1	37	129
NetAmsa	1	6	39
mAMSA	3	60	165
SN 16713	3	35	100
NetAmsa	3	4	25
In the presence of DNA			
mAMSA	3	6.5	44
SN 16713	3	6	108
NetAmsa	3	10	60
pH 7.0			
mAMSA	3	>1200	
SN 16713	3	840	>1200
NetAmsa	3	390	>1200

$t_{1/2}$ and t correspond to the time necessary for half and complete oxidation of the ligand, respectively.

The kinetics of oxidation were also analyzed in the presence of calf thymus DNA. The time necessary for complete oxidation of SN 16713 is practically identical in the absence and presence of DNA. In contrast, the addition of DNA significantly affects the kinetics of oxidation of mAMSA and NetAmsa. As indicated in Table 1, the copper-dependent oxidation of mAMSA proceeds much more rapidly in the presence of DNA, whereas that of NetAmsa becomes slower. These effects may tentatively be correlated with the stability of the drug/DNA complexes. mAMSA, which can dissociate most rapidly from the double helix, is very susceptible to oxidation in the presence of DNA. Conversely, NetAmsa/DNA complexes dissociate very slowly (13); as a consequence, the anilino-acridine portion of the hybrid may be less accessible for oxidation. However, the reason why DNA should accelerate oxidation of mAMSA is not clear.

Measurements of reactive oxygen metabolites by chemiluminescence. Mechanistic studies of DNA strand breakage by mAMSA in the presence of copper have established that molecular oxygen is required for efficient activation and suggest that superoxide free radicals ($O_2^{\cdot-}$) but not hydroxyl radicals ($OH^{\cdot}$) are involved in the DNA cleaving reaction (18, 19). To determine whether superoxide radicals are effectively produced during the oxidation process, we resorted to a chemiluminescence assay based on the capacity of lucigenin to react specifically with $O_2^{\cdot-}$ and/or H_2O_2 but not with $OH^{\cdot}$ (26). A brief description of the reductive dioxygenation of lucigenin in the presence of $O_2^{\cdot-}$ or H_2O_2 is given in Materials and Methods. As indicated, the amount of light produced during the chemiluminescence reaction is directly proportional to the quantity of reactive oxygen species produced and therefore, in the current situation, to the rate of oxidation of mAMSA and its derivatives by copper ions.

Fig. 6 shows the chemiluminescence responses recorded during the copper-dependent oxidation of the drugs at pH 9.4. In the absence of copper ions (Fig. 6a), NetAmsa produces slightly less oxygen radical species than mAMSA and SN 16713. Conversely, in the presence of Cu(II) (Fig. 6b), the chemiluminescence intensity is notably weaker with mAMSA than with the two 4-carboxamide derivatives. The chemiluminescence reaction, which is presumptive of the production of oxygen radicals, proceeds more rapidly with NetAmsa than with SN 16713. The results are fully consistent with the oxidation kinetics. mAMSA oxidizes much more slowly in the presence of copper than does NetAmsa and consequently generates less oxygen-based free radicals than the combilexin.

Copper-dependent DNA cleavage. In a first set of experiments, strand scission was analyzed by monitoring the conversion of supercoiled plasmid DNA (form I) to nicked circular molecules (form II) and linear DNA (form III). The tests were performed using an equimolar concentration of drug and copper (Fig. 7, *top*) as well as with a fixed drug concentration and increasing concentrations of copper (Fig. 7, *bottom*). In both cases, DNA/drug/Cu(II) complexes were incubated for 6 hr at room temperature in 50 mM Na borate buffer, pH 9.4, before electrophoresis. The gels in Fig. 7 show that DNA cleavage is slightly more efficient with NetAmsa

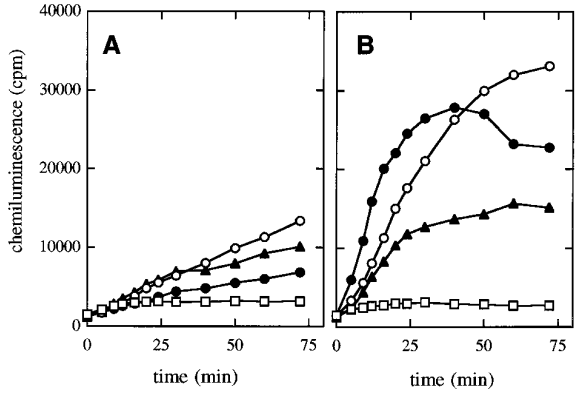

Fig. 6. Chemiluminescent responses of mAMSA (▲), SN 16713 (○), and NetAmsa (●) (100 μM each) in the absence (A) and presence (B) of 10 μM copper. Reactions were conducted in 50 mM sodium borate, pH 9.4, in the presence of 100 μM lucigenin as chemiluminescent probe. □, Control sample containing lucigenin plus copper in the absence of drug.

than with mAMSA. At a high concentration of NetAmsa (150 μM), >90% of the DNA is converted to linear molecules (form III), whereas under the same conditions, only ~25% linear DNA is produced with mAMSA. NetAmsa and SN 16713 (i.e., the two DNA-threading agents) exhibit approximately similar DNA cleaving capacities. The results are consistent with the oxidation kinetics (Table 1) and the chemiluminescence data (Fig. 6).

The next problem was to determine whether the strand breaks induced by NetAmsa occur at specific sequences in DNA. To answer this question, a detailed analysis of the DNA sequences cut in the presence of NetAmsa was performed by studying the copper-dependent scission of DNA using sequencing gels. Cleavage sites were sequenced using a 5′-end-labeled *Ava*I/*Pvu*II restriction fragment from pBS DNA (265 bp long) that contains several AT-rich sites preferentially recognized by NetAmsa, as determined on the basis of footprinting experiments using DNase I and MPE·Fe(II) as cleaving agents (Fig. 8). The combined use of an enzyme and a chemical nuclease permits both sensitive and accurate location of drug-binding sites in DNA (27). The positions of five binding sites around positions 55, 65, 78, 95, and 126 were accurately determined within the entire length of the 265-bp sequence accessible to densitometric analysis. The sequences protected from cleavage by the nuclease are 5′-TTTTG, 5′-TTTAG, 5′-AATTT, 5′-AATCA, and 5′-AAATTGTTAT. Except for the last region, which most likely corresponds to two juxtaposed binding sites, the sites are 5 bp long, as predicted on the basis of the molecular modeling analysis (Fig. 5). Additional footprinting experiments were performed with an 81-bp *Eco*RI/*Hin*dIII fragment from plasmid pTLX, which contains a long polypurine/polypyrimidine tract for triple-helix formation (29). The comparison of the footprints obtained with NetAmsa and its parent compounds netropsin and SN 16713 (Fig. 9) reveals unambiguously that NetAmsa retained the AT selectivity conferred by the netropsin moiety, which is in agreement with other results reported recently (13).

The same 265-mer fragment used for footprinting was allowed to react with NetAmsa in the presence of copper in borate buffer, pH 9.4. A typical gel showing the cleavage products resulting from a 5-hr incubation of the DNA with the NetAmsa/copper redox system is shown in Fig. 10A. Under the chosen experimental conditions, the DNA remains uncleaved in the absence of drug and presence of copper or in the presence of drug and absence of copper. When both NetAmsa and Cu(II) are present in the reaction mixture, cleavages can be detected at various positions in the sequence. The nucleotide sequences that are most sensitive to the drug do not coincide with the binding sites inferred from the footprinting experiments. Although cleavages occur predominantly at certain sites, such as the GC-rich tract at positions 69–71, the cutting is not restricted to specific sequences and seems to occur nonspecifically at a high drug concentration. However, a closer inspection of the most intense breaks indicates that C residues and, to a lesser extent, G residues are preferentially attacked. Within the 265-mer fragment, positions C33, C36, C60, G69, G71, C85, and C102 are particularly susceptible to cutting by the drug/copper complex. These experiments were repeated several times, and the same cutting sites were consistently observed. The extent of cleavage was found to be higher when the DNA was

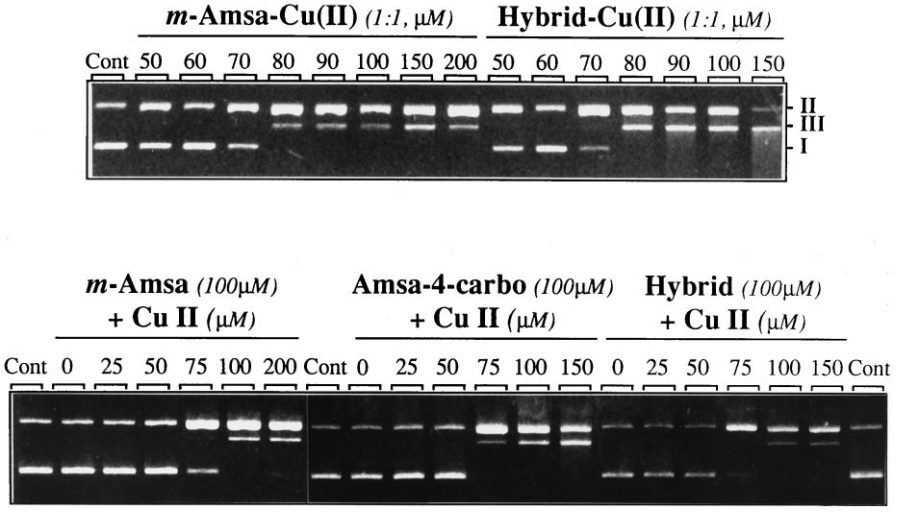

Fig. 7. Cleavage of closed circular pBS DNA (*form I*) by mAMSA, SN 16713, and the hybrid molecule. The plasmid DNA was incubated with increasing drug concentrations in the presence of an equimolar concentration of $CuSO_4$ (*top*) or with 100 μM drug and increasing concentrations of copper (*bottom*). *Forms II and III*, nicked and linear DNA forms, respectively. *Top of each lane*, drug concentration (μM). *Cont*, plasmid DNA incubated without drug and copper. Reactions were performed in 50 mM sodium borate buffer, pH 9.4, for 6 hr at room temperature in the dark.

reacted with the drug/copper complex for longer periods at basic pH, but the same cutting sites were still detected (Fig. 10B). The extent of cutting was significantly reduced when the reaction was performed at pH 7.0, data not shown. At neutral pH, the oxidation of the conjugate in the presence of copper is slow (Table 1); consequently, fewer oxygen radicals and DNA breaks are generated.

The intriguing observation that the copper-dependent breaks occur predominantly at C and G residues prompted us to investigate further the cutting reaction with other DNA fragments, such as the 117-bp restriction fragment from plasmid pBS that we employed in a previous DNA-binding study (13). This restriction fragment, which offers five AT-rich binding sites for the hybrid compound, was also exposed to attack by the conjugate in the presence of copper under alkaline conditions (Fig. 11). Again, it seems that (i) the cutting sites are not restricted to the favored binding sites inferred from footprinting experiments and (ii) copper-dependent cleavage occurs selectively at C residues and sometimes at G residues.

Topoisomerase-mediated DNA cleavage. The effects of the hybrid and its parent compounds were initially tested on purified calf thymus topoisomerases I and II using a ^{32}P-labeled *Eco*RI/*Hin*dIII restriction fragment of pBR322 as substrate. The DNA cleavage products were analyzed by agarose gel electrophoresis under alkaline conditions (for topoisomerase I) or in neutral buffer (for topoisomerase II). Autoradiographs of typical gels obtained after treatment of the 4330-bp DNA substrate with topoisomerases I and II in the presence and absence of the test drugs at concentrations of 0.1–100 μM are shown in Fig. 12.

It was the observation that minor groove binders such as netropsin and distamycin can affect the reaction of topoisomerase I with DNA (30) that prompted us to determine whether the NetAmsa conjugate can interfere with the topoisomerase I reaction in addition to the expected effect on topoisomerase II. Purified topoisomerase I produces a characteristic cleavage pattern in the absence of drug. Slightly modified electrophoretic profiles were observed in the presence of our compounds. The cleavage seems to be stimulated at only one particular site (Fig. 12A, *arrowheads*) with all three drugs tested. The stimulation is very weak compared with that observed with the topoisomerase I-specific inhibitor camptothecin. It is clear that netropsin as well as the anilino-acridine derivatives have little, if any, effect on topoisomerase I.

It is well established that in the presence of topoisomerase II and DNA, mAMSA stabilizes the enzyme/DNA interaction in the form of a "cleavable complex." In this complex, the enzyme is covalently linked to the 5′-end of the DNA so that treatment with a detergent (e.g., SDS) results in the formation of strand breaks, which can be revealed by gel electrophoresis of the DNA fragments. To determine whether the linkage of the netropsin moiety affects the capacity of mAMSA to form cleavable complexes, the same ^{32}P-labeled *Eco*RI/*Hin*dIII restriction fragment was used as a substrate for purified calf topoisomerase II. The patterns of double-strand cleavage are shown in Fig. 12B. As expected, mAMSA and, to a lesser extent, SN 16713 strongly stimulate DNA cleavage by topoisomerase II at defined sites. NetAmsa seems to be less efficient. A weak but noticeable effect can be detected with NetAmsa at concentrations of ≥10 μM, whereas there is no detectable effect with netropsin even at a concentration as high as 100 μM. The cleavage patterns observed with SN 16713 and mAMSA are slightly different, indicating that the 4-carboxamide side chain plays a role in the interference with the enzyme. The few topoisomerase II cutting sites stimulated by NetAmsa (Fig. 12B, *arrowheads*) are found with mAMSA. Therefore, it seems that NetAmsa remains capable of inhibiting the reaction of topoisomerase II with DNA, although the effect is rather modest compared with what can be achieved with the parent drug mAMSA. The linkage of the netropsin moiety, which confers marked sequence-selective recognition properties, is evidently detrimental to the effect on topoisomerase II.

Sequencing of drug-stimulated DNA cleavage by topoisomerase II. The next question that we considered was whether the netropsin moiety appended to the topoisomerase II-targeted domain of NetAmsa serves to direct the intensity and location of DNA cleavage sites. Both 5′-end-labeled 117- and 265-bp *Eco*RI/*Pvu*II restriction fragments from pBS used in the copper-dependent DNA cleavage experiments were used as substrates for purified calf thymus or human topoisomerase II (the p170 form commercially available). DNA cleavage patterns resulting from enzyme-mediated double-strand breaks stimulated by the two drugs were studied at

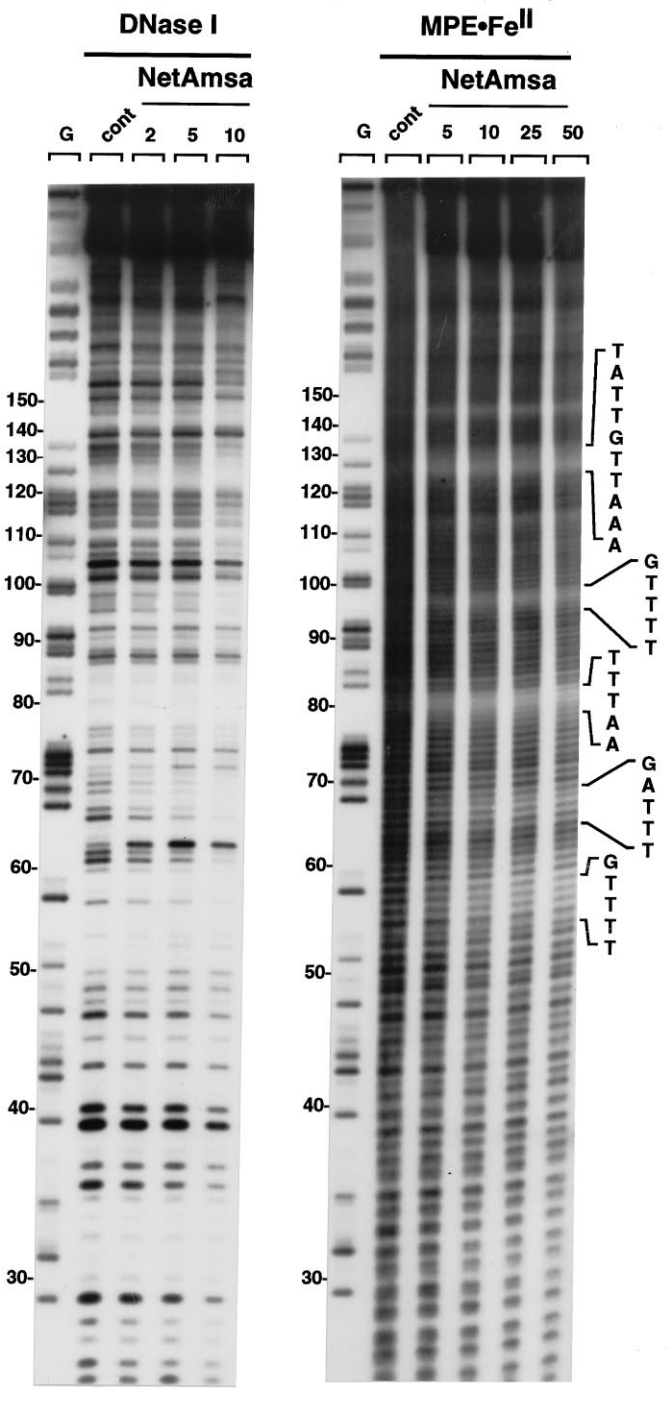

Fig. 8. DNase I (*left*) and MPE·Fe(II) (*right*) footprinting with the 5′-labeled 265-mer *Pvu*II/*Eco*RI restriction fragment of the plasmid pBS in the presence of different concentrations of the netropsin/mAMSA hybrid. The DNA was 5′-end labeled at the *Eco*RI site with [γ-^{32}P]ATP in the presence of T4 polynucleotide kinase. The products of nuclease digestion were resolved on an 8% polyacrylamide gel containing 7 M urea. *Top of each lane*, concentration (μM) of the drug tested. Control tracks (*Cont*) contained no drug. *G*, Maxam-Gilbert sequencing marker lanes specific for guanine residues. *Numbers on the left*, standard numbering scheme for the nucleotide sequence of the DNA fragment. *Sequences on the right*, location of the footprints at AT-rich sites.

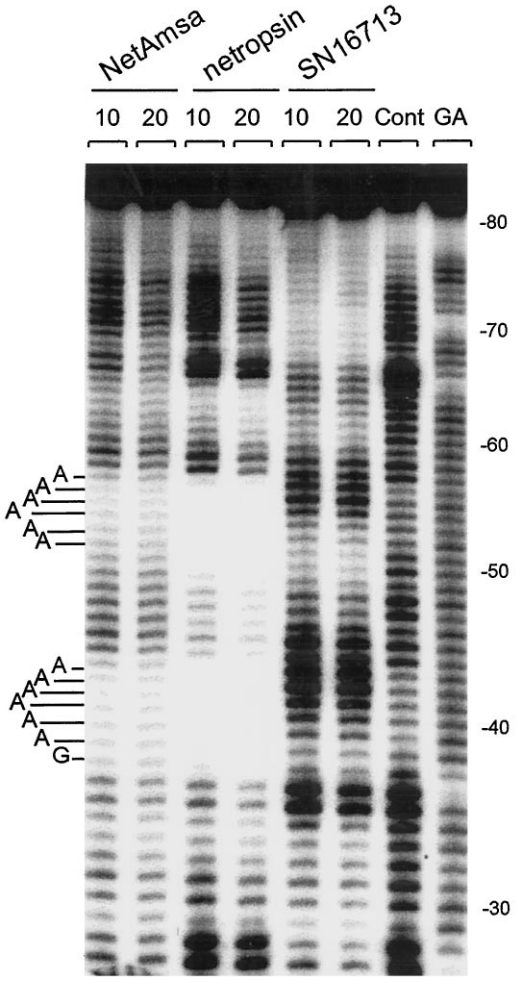

Fig. 9. DNase I footprinting with the 3′-labeled 81-mer *Hin*dIII/*Eco*RI restriction fragment of the plasmid pTLX (29) in the presence of SN 16713, netropsin, and NetAmsa. The DNA was 3′-end labeled at the *Eco*RI site with [α-^{32}P]dATP in the presence of avian myeloblastosis virus reverse transcriptase. *GA*, sequencing markers specific for purine residues. Other details are given in the legend for Fig. 8.

different concentrations. With the 117-mer fragment, three topoisomerase II-mediated cutting sites were stimulated in the presence of NetAmsa and mAMSA (Fig. 13, arrows). The patterns of DNA cleavage induced by topoisomerase II in the presence of either drug are identical, and no differences could be detected using the calf or human enzymes. Apparently, despite their structural differences, these two anilinoacridine derivatives modulate the catalytic activity of the enzyme in an approximately comparable manner. Both stimulate DNA cleavage by the enzyme at positions 13 (5′-ATAG ↓ TGAG), 24 (5′-TATT ↓ ACAA), and 97 (5′-TTGC ↓ AGCA) on the 117-mer fragment. On the 265-mer fragment (data not shown), two topoisomerase II cleavage sites enhanced by the drugs were located at positions 41 (5′-CTGC ↓ AGGC) and 95 (5′-GTAA ↓ TCAT) (two other sites were visible at the top of the gel, but they lie beyond the portion of the sequence accessible to analysis). It seems, however, that the netropsin moiety does exert some influence on the process; with mAMSA, the extent of cleavage remained constant over the concentration range tested, whereas with the hybrid compound, the reaction was stimulated at a low drug concentration but inhibited at a high concentration ($\geq$50 μM). Inhibition of cutting at high concentrations is a common property of DNA-intercalating drugs. The results confirm that the netropsin moiety of the hybrid reduces but does not prevent stimulation of DNA cleavage by topoisomerase II. It is very likely that the bis-

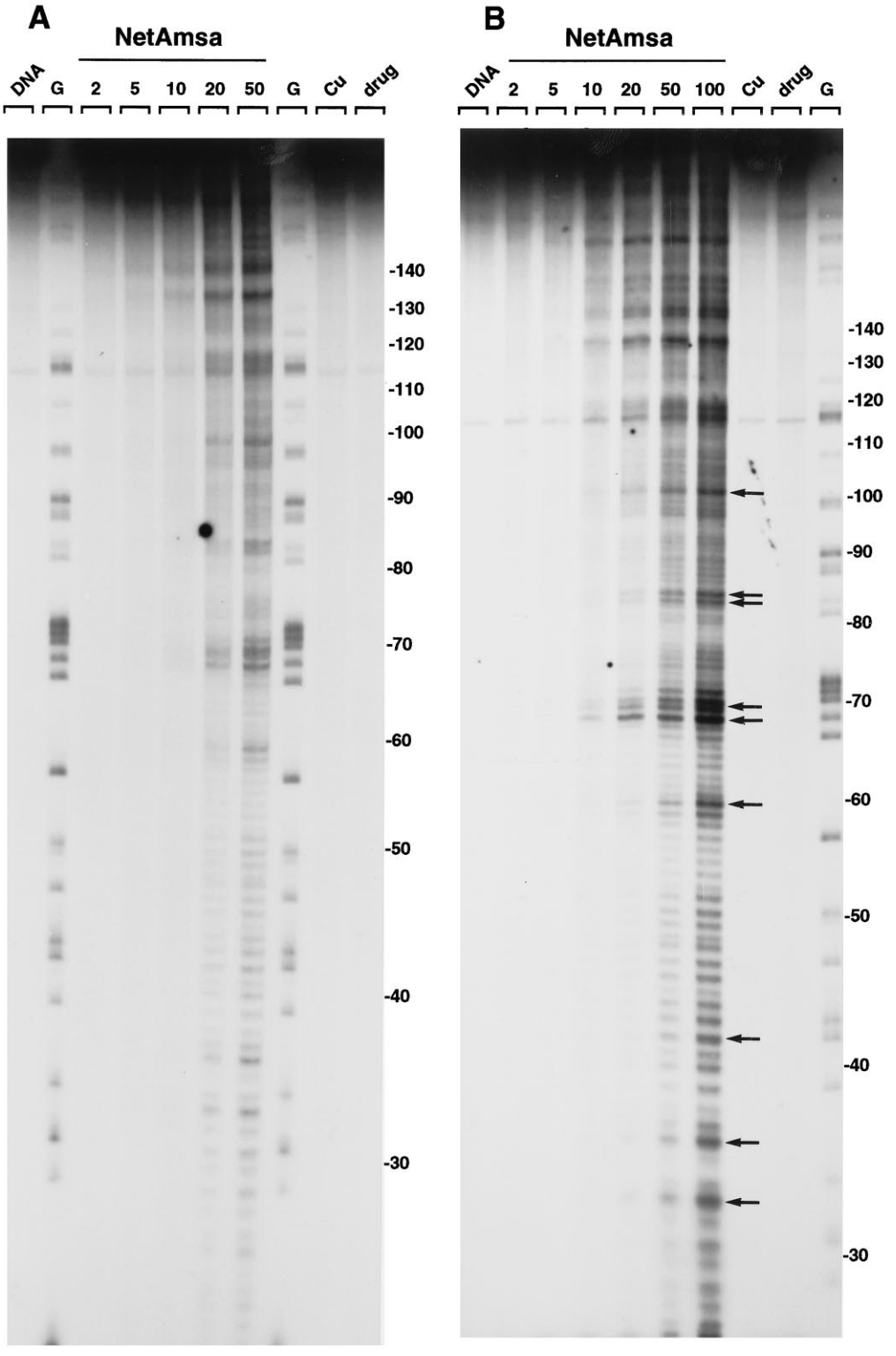

Fig. 10. Copper-dependent cleavage of DNA with NetAmsa. The 265-mer DNA fragment labeled at the 5′-end of the *Eco*RI site was reacted with increasing concentrations of the netropsin/mAMSA hybrid in the presence of 200 μM $CuSO_4$. Reactions were conducted in 50 mM sodium borate buffer, pH 9.4, for 5 hr (A) and 15 hr (B). Samples were subsequently lyophilized and then electrophoresed onto an 8% denaturing polyacrylamide gel. *DNA* and *Cu*, control DNA in the absence and presence of 200 μM $CuSO_4$, respectively, subjected to the same treatment at pH 9.4 in the absence of drug. *G*, Guanine-specific sequence markers obtained by treatment of the DNA with dimethylsulfate-piperidine. *Arrows*, nucleotides with which the hybrid compound reacted strongly.

pyrrole moiety is not involved in direct interaction of the drug with the enzyme. The 1′-substituent on the anilino ring (the methanesulfonamido group) is presumed to provide the topoisomerase II-binding domain (31).

The possibility that mAMSA and NetAmsa affect the association or dissociation of topoisomerase II/DNA complexes differently was examined, but no significant differences between the two drugs were observed. The kinetics of appearance (Fig. 14A) and reversal (Fig. 14B) of topoisomerase II-mediated DNA cleavage sites are very similar in the presence of mAMSA and NetAmsa. The results confirm that the netropsin moiety of the hybrid exerts little, if any, effect on the activity of the hybrid toward topoisomerase II *in vitro*.

Discussion

The netropsin/mAMSA combilexin threads through the DNA double helix so as to intercalate its acridine chro-

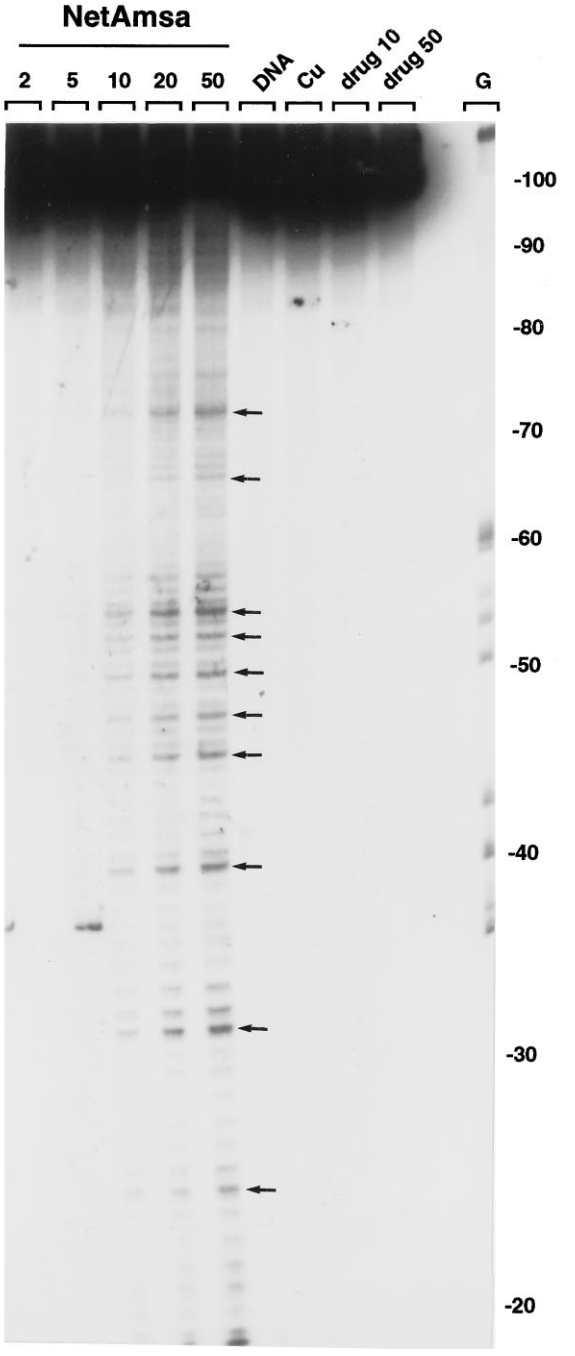

Fig. 11. Copper-dependent cleavage of the 117-mer DNA fragment. The DNA (5′-end labeled) was reacted with the netropsin/mAMSA hybrid in the presence of 200 μM $CuSO_4$. Reactions were conducted in 50 mM sodium borate buffer, pH 9.4, for 15 hr at 37°. Other details are given in legend for Fig. 10.

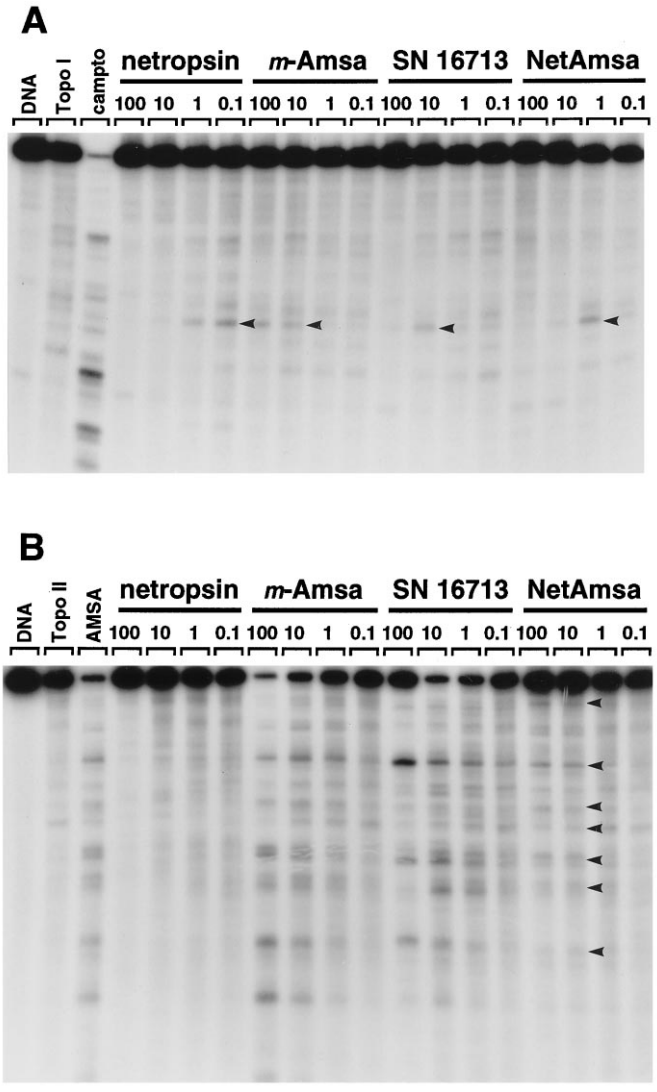

Fig. 12. Effects of drugs on topoisomerase I (A) and topoisomerase II (B). Purified calf thymus topoisomerase I or II was incubated with the *Eco*RI/*Hin*dIII restriction fragment from pBR322 (^{32}P-labeled at the *Eco*RI site) in the presence or absence of the test ligands. *Top of each lane*, drug concentration (μM). Reactions were carried out for 10 min at 37° and then stopped with SDS/proteinase K treatment. A, Single-stranded DNA fragments were analyzed on a 1% alkaline agarose gel in TBE buffer. *DNA* and *Topo I*, radiolabeled 4330-bp DNA substrate incubated without and with topoisomerase I, respectively. Camptothecin (*campto*) was used at 0.03 μM. B, Double-stranded DNA fragments were analyzed on a 1% neutral agarose gel in TBE buffer. *Topo II*, topoisomerase II. *Arrowheads*, principal site of topoisomerase I cleavage stimulated by all four drugs tested (A) and sites of topoisomerase cleavage stimulated by NetAmsa (B).

mophore, leaving the netropsin moiety and the methanesulfonanilino group positioned within the minor and major grooves of the double helix, respectively. The DNA-threading process takes place preferentially at AT-rich sequences (13). In the current study, we showed through the use of complementary biochemical methods that NetAmsa has retained two fundamental properties of mAMSA: (i) the inhibition of topoisomerase II and (ii) the oxidation-dependent production of free radicals responsible for DNA breakage. Linkage of the netropsin moiety to mAMSA slightly reduces but does not abolish the capacity of the intercalator to interfere with the catalytic activity of topoisomerase II. On the other hand, the presence of a 4-carboxamide side chain confers on the drug a higher susceptibility to copper-dependent oxidation to a quinone imine form. Therefore, both the combilexin molecule and mAMSA are capable of triggering DNA breakage via two distinct mechanisms, one of which is dependent on metabolic activation of the drug and one of which requires the functioning of a ubiquitous enzyme. The retention of these two characteristics that are believed to be responsible for the antitumor activity of mAMSA served to justify biological studies. Preliminary tests *in vitro* indicate that NetAmsa is cytotoxic

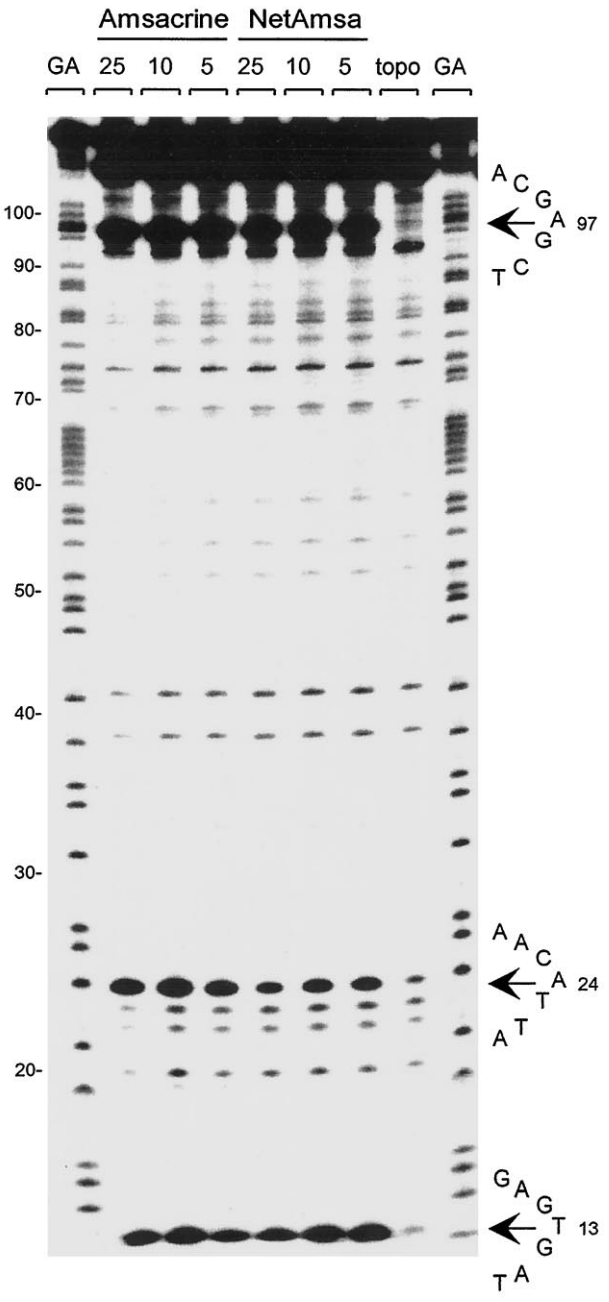

Fig. 13. Sequence analysis of the topoisomerase II (*topo*) cleavage sites stimulated by NetAmsa and mAMSA. The 5′-end-labeled 117-mer fragment from plasmid pBS was incubated in the absence (*Topo*) or presence of 10, 20, or 50 μM mAMSA or NetAmsa. Fragments were separated on an 8% denaturing polyacrylamide gel. *Numbers at the left*, nucleotide position, determined with reference to the purine nucleotide tracks (*GA*). *Arrows*, three major topoisomerase II-mediated break points.

toward murine leukemia (L1210) and human lymphoblast (Molt4/C8 and CEM/0) cell lines.[1] However, neither interference with topoisomerase II nor redox activation is sufficient to guarantee antitumor activity. The design of active antitumor drugs is a difficult exercise that requires not only consideration of the interaction between the drug and its potential targets but also a wide range of independent parameters, including cellular uptake/efflux and drug distribution. Nevertheless, there are strong grounds for the belief that the development of combilexin molecules such as that reported in the present study will afford a successful approach to the design of new DNA-cleaving antitumor agents, although it is evident that some problems remain to be solved at the level of drug/DNA interaction. In that regard, the study of NetAmsa will provide information that is useful in the design of compounds. For example, it is clearly not sufficient to link two well-characterized moieties, each of which has exemplary characteristics in isolation; the nature and positioning of the linkage may have to be varied.

There is no obvious correlation between the preferred NetAmsa-binding sites inferred from footprinting experiments and the DNA-cleavage sites, whether topoisomerase II-mediated or oxidation-associated strand breaks (Fig. 15). The netropsin moiety plays its expected role in driving the mAMSA chromophore to AT sequences in DNA, but the sequence-selectivity of topoisomerase II-mediated cleavage is not affected. The footprints clearly correspond to AT-rich sites at which both the netropsin and the mAMSA moiety of NetAmsa are engaged in interaction with DNA, as shown previously (bidentate binding) (13). Although the evidence is strong that the conjugate behaves as a DNA-threading agent (13), it is nevertheless hard to exclude the possibility that a fraction of the drug molecules can either bind to the minor groove or intercalate but fail to do both simultaneously. In particular, there is a real possibility that some hybrid molecules could bind to non-AT-rich sequences via intercalation of the acridine ring with the appended bis-pyrrole standing clear of the bases on the floor of the minor groove (monodentate binding). The coexistence of different binding processes was previously demonstrated with other combilexin molecules (10, 32). Because the molecular contacts between topoisomerase II and DNA take place mainly in the major groove (33), the enzyme may not distinguish between bidentate and monodentate binding since in both cases, the methanesulfonamido group (i.e., the topoisomerase II-targeted domain) would protrude similarly toward the major groove regardless of whether the netropsin tail was anchored in the opposite minor groove. This could well account for much of the lack of correlation between strong footprints and cleavage sites. It is also possible that the netropsin tail has a guenine tendency to impede full intercalation of the hybrid chromophore, which would contribute to the observed lower activity against topoisomerase II. Similar arguments can be applied to account for the results of copper-dependent cleavage. Free radicals generated in the vicinity of the oxidized portion of the hybrid (i.e., the anilino ring projecting into the major groove) could attack the DNA bases independently of the position of the netropsin moiety. Furthermore, $OH^{\bullet}$ radicals can be produced before the drug gains access to its preferred binding sites, and they can also diffuse around those sites to engender quasi-random strand cleavages. However, the fact that copper-dependent cleavages occur preferentially at single residues (C and sometimes G) suggests the operation of nondiffusing oxidized species and a mechanism that would implicate deoxyribose modification, as has been demonstrated with drug/metal complexes. Further studies will be needed to validate or refute these hypotheses.

This is not the only study that has failed to find a correlation between the sequence selectivity of drug binding to (pro-

[1] E. De Clercq, unpublished observations.

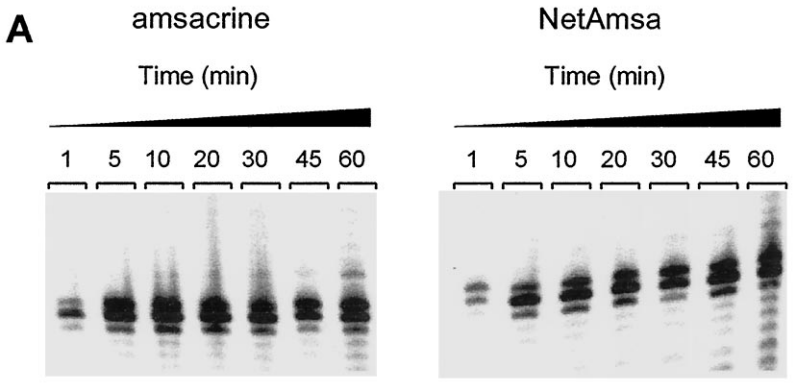

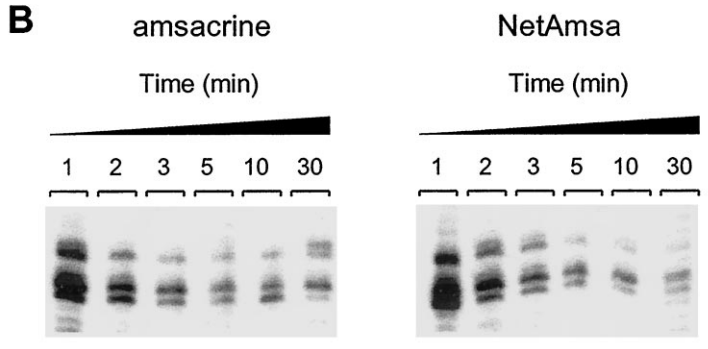

Fig. 14. Kinetics of formation (A) and reversal (B) of mAMSA and NetAmsa-induced cleavage sites at positions 46–47 of the 265-mer fragment from plasmid pBS. A, Topoisomerase II was added to the drug/DNA complex, and the reaction was stopped at intervals by the addition of SDS/proteinase K. B, A 50-fold excess of unlabeled DNA was added at intervals to induce the dissociation of cleavable complexes before the addition of SDS/proteinase K to stop the reaction. In control experiments, the addition of unlabeled DNA before the enzyme completely prevented the formation of cleavable complexes (not shown).

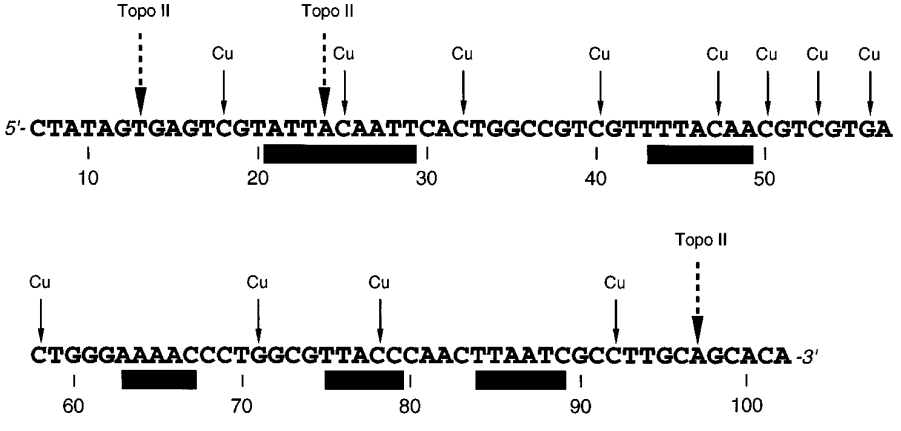

Fig. 15. Diagrammatic representation of the footprints and copper-dependent or topoisomerase II (*Topo II*)-mediated strand cleavages produced by the hybrid molecule on the 5′-end-labeled 117-mer fragment. Only the region of the restriction fragment that was analyzed by densitometry is shown. *Underlined sequences*, position of the footprints [i.e., positions of inhibition of DNase I and MPE·Fe(II) cutting by NetAmsa] and therefore the putative reversible binding sites. *Dashed arrows*, sites of topoisomerase II-mediated DNA cleavage. *Solid arrows*, main copper-dependent strand breaks.

tein-free) DNA and effects on topoisomerase II. Daunomycin binds preferentially to A/TGC and A/TCG triplets (3), whereas daunomycin-induced topoisomerase II strand breaks can occur at many types of sites not necessarily encompassing the aforementioned triplets. The presence of an adenine residue at position -1 relative to the cleavage site (T at +5) is the only requirement for daunomycin-stabilized cleavage of DNA by topoisomerase II (34). Actinomycin exhibits a sharp selectivity for CpG-containing sites (4), but no specific sequence requirement for topoisomerase II inhibition has been reported. Conversely, cleavage sites produced by topoisomerase II in response to epipodophyllotoxins and quinolone derivatives show a preponderance of C at the -1 position (35, 36), whereas these drugs interact loosely, if at all, with DNA in the absence of the enzyme. In nearly all cases, it seems that the known sequence selectivity of drug binding to DNA has little to do with the location of drug-induced topoisomerase II breaks. Binding to DNA and topoisomerase inhibition may be viewed as two distinct molecular processes that contribute separately to the cytotoxic activity. Furthermore, it is clear that antitumor activity must demand more than complex formation between the drugs and GC- or AT-rich sequences in DNA together with specific induction of DNA strand breaks via topoisomerase II. There are grounds for the belief that it is the effect on DNA secondary structure, not the primary sequence selectivity, that is important for interference with the catalytic activities of topoisomerases. The distinctive localized structural perturbations of base-

pairing and helix conformation induced by intercalating drugs such as mAMSA, daunomycin, and actinomycin quite possibly represent the overriding factor responsible for their specific effects on topoisomerase II. DNA structure is known to influence the functioning of the enzyme (37). Combilexin molecules such as NetAmsa may also operate by specifically modulating the local conformation of DNA.

It is important to bear in mind that the topoisomerase II cleavage sites determined in the current study with NetAmsa or with any other drugs *in vitro* could be different from those that occur in cells. It seems that for the epipodophyllotoxin VM-26, it is chromatin structure, not DNA sequence specificity alone, that is the primary determinant of topoisomerase II sites of action *in vivo* (38). Although drugs can maintain a high degree of sequence specificity in binding to chromatin of living cells, corresponding to that established *in vitro*, recent studies suggest that it may be the genomic site and reversion kinetics of DNA cleavage *in vivo* that are the primary factors influencing cytotoxic potency (39). Studies are in progress to investigate site-specific DNA cleavage by NetAmsa in cells.

References

1. Kamitori, S., and F. Takusagawa. Multiple binding modes of anticancer drug actinomycin D: x-ray, molecular modeling, and spectroscopic studies of d(GAAGCTTC)$_2$-actinomycin D complexes and its host DNA. *J. Am. Chem. Soc.* **116:**4154–4165 (1994).
2. Frederick, C. A., L. D. Williams, G. Ughetto, G. A. van der Marel, J. H. van Boom, A. Rich, and A. H.-J. Wang. Structural comparison of anticancer drug-DNA complexes: adriamycin and daunomycin. *Biochemistry* **29:** 2538–2549 (1990).
3. Chaires, J. B., J. E. Herrera, and M. J. Waring. Preferential binding of daunomycin to 5′(A/T)CG and 5′(A/T)GC sequences revealed by footprinting titration experiments. *Biochemistry* **29:**6145–6153 (1990).
4. Bailly, C., G. Ridge, D. E. Graves, and M. J. Waring. Use of a photoactive derivative of actinomycin D to investigate shuffling between binding sites on DNA. *Biochemistry* **33:**8736–8745 (1994).
5. Waring, M. J. Echinomycin and related quinoxaline antibiotics, in *Molecular Aspects of Anticancer Drug-DNA Interactions* (S. Neidle and M. J. Waring, eds.). Vol 1. Macmillan, Basingstoke/London, 213–242 (1993).
6. Gao, X., A. Stassinopoulos, J. S. Rice, and I. H. Goldberg. Structural basis for the sequence-specific DNA strand cleavage by the enedyine neocarzinostatin chromophore: structure of the post-activated chromophore-DNA complex. *Biochemistry* **34:**40–49 (1995).
7. Bailly, C., and J. P. Hénichart. Molecular pharmacology of intercalator-minor groove binder hybrid groove binder hybrid molecules, in *Molecular Aspects of Anticancer Drug-DNA Interactions* (S. Neidle and M. J. Waring, eds.). Vol. 2. Macmillan, London, 162–196 (1994).
8. Cassileth, P. A., and R. P. Gale. Amsacrine: a review. *Leukemia Res.* **10:**1257–1265 (1986).
9. Ralph, R. K., W. Judd, Y. Pommier, and K. W. Kohn. DNA topoisomerases, in *Molecular Aspects of Anticancer Drug-DNA Interactions* (S. Neidle and M. J. Waring, eds.). Vol. 2. Macmillan, London, 1–95 (1993).
10. Bailly, C., C. Michaux, P. Colson, C. Houssier, J. S. Sun, T. Garestier, C. Hélène, J. P. Hénichart, C. Rivalle, E. Bisagni, and M. J. Waring. Reaction of a biscationic distamycin-ellipticine hybrid ligand with DNA: mode and sequence specificity of binding. *Biochemistry* **33:**15348–15364 (1994).
11. Bailly, C., M. Collyn-d'Hooghe, D. Lantoine, C. Fournier, B. Hecquet, P. Fossé, J. M. Saucier, P. Colson, C. Houssier, and J. P. Hénichart. Biological activity and molecular interaction of a netropsin-acridine hybrid ligand with chromatin and topoisomerase II. *Biochem. Pharmacol.* **43:**457–466 (1992).
12. Bailly, C., W. A. Denny, L. Mellor, L. P. G. Wakelin, and M. J. Waring. Sequence-specificity of the binding of 9-aminoacridine- and amsacrine-4-carboxamides to DNA studied by DNase I footprinting. *Biochemistry* **31:** 3514–3524 (1992).
13. Bourdouxhe-Housiaux, C., P. Colson, C. Houssier, M. J. Waring, and C. Bailly. Interaction of a DNA-threading netropsin-amsacrine combilexin with DNA and chromatin. *Biochemistry* **35:**4251–4264 (1996).
14. van Houte, L. P. A., C. J. van Garderen, and D. J. Patel. The antitumor drug nogalamycin forms two different intercalation complexes with d(GCGT)•d(ACGC). *Biochemistry* **32:**1667–1674 (1993).
15. Hansen, M. R., and L. Hurley. Pluramycins. Old drugs having modern friends in structural biology. *Acc. Chem. Res.* **29:**249–258 (1996).
16. Shoemaker, D. D., R. L. Cysyk, S. Padmanabhan, H. B. Bhat, and L. Malspeis. Identification of the principal biliary metabolite of 4′-(9-acridinylamino)methanesulfon-*m*-anisidide in rats. *Drug Metab. Dispos.* **10:**35–39 (1982).
17. Kettle, A. J., I. G. C. Robertson, B. D. Palmer, R. F. Anderson, K. B. Patel, and C. C. Winterbourn. Oxidative metabolism of amsacrine by the neutrophil enzyme myeloperoxidase. *Biochem. Pharmacol.* **44:**1731–1738 (1992).
18. Wong, A., C.-H. Huang, and S. T. Crooke. Deoxyribonucleic acid breaks produced by 4′-(9-acridinylamino)methanesulfon-*m*-anisidide and copper. *Biochemistry* **23:**2939–2945 (1984).
19. Wong, A., C.-H. Huang, and S. T. Crooke. Mechanism of deoxyribonucleic acid breakage induced by 4′-(9-acridinylamino)methanesulfon-*m*-anisidide and copper: role for cuprous ion and oxygen free radicals. *Biochemistry* **23:**2946–2952 (1984).
20. Robbie, M. A., B. D. Palmer, W. A. Denny, and W. R. Wilson. The fate of $N^{1\prime}$-methanesulphonyl-$N^{4\prime}$-(9-acridinyl)-3′-methoxy-2′:5′-cyclohexadiene-1′,4′-diimine (*m*-AQDI), the primary oxidative metabolite of amsacrine, in transformed Chinese hamster fibroblast. *Biochem. Pharmacol.* **39:**1411–1421 (1990).
21. Covey, J. M., K. W. Kohn, D. Kerrigan, E. J. Tilchen, and Y. Pommier. Topoisomerase II-mediated DNA damage produced by 4′-(9-acridinylamino)methanesulfon-m-anisidide and related acridines in L1210 cells and isolated nuclei: relation to cytotoxicity. *Cancer Res.* **48:**860–865 (1988).
22. Gorsky, L. D., and M. J. Morin. Microsomal activation and increased production of 4′-(9-acridinylamino)-3-methanesulfon-*m*-anisidide (m-AMSA)-dependent, topoisomerase-associated DNA lesions in nuclei from human HL-60 leukemia cells. *Biochem. Pharmacol.* **39:**1481–1484 (1990).
23. Wakelin, L. P. G., P. Chetcuti, and W. A. Denny. Kinetic and equilibrium binding studies of amsacrine-4-carboxamides: a class of asymmetrical DNA-intercalating agents which bind by threading through the DNA helix. *J. Med. Chem.* **33:**2039–2044 (1990).
24. Houssin, R., J. L. Bernier, J. P. Hénichart. A convenient and general method for the preparation of tert-butoxycarbonylaminoalkanenitriles and their conversion to mono-tert-butoxycarbonylalkanediamines. *Synthesis* **3:**259–261 (1988)
25. Bailly, C., N. Pommery, R. Houssin, and J. P. Hénichart. Design, synthesis, DNA-binding, and biological activity of a series of DNA minor groove binding intercalating drugs. *J. Pharm. Sci.* **78:**910–917 (1989).
26. Allen, R. C. Phagocytic leukocyte oxygenation activities and chemiluminescence: a kinetic approach to analysis. *Methods Enzymol.* **133:**449–493 (1986).
27. Bailly, C., and M. J. Waring. Comparison of different footprinting methodologies for detecting binding sites for a small ligand on DNA. *J. Biomol. Struct. Dyn.* **12:**869–898 (1995).
28. Pommier, Y., G. Capranico, A. Orr, and K. W., Kohn. Distribution of topoisomerase II cleavage sites in Simian virus 40 DNA and the effects of drugs. *J. Mol. Biol.* **222:**909–924 (1991).
29. Marchand, C., C. Bailly, C. H. Nguyen, E. Bisagni, T. Garestier, C. Hélène, and M. J. Waring. Stabilization of triple helical DNA by a benzopyridoquinoxaline intercalator. *Biochemistry* **35:**5022–5032 (1996).
30. Chen, A. Y., C. Yu, B. Gatto, and L. F. Liu. DNA minor groove-binding ligands: a different class of mammalian DNA topoisomerase I inhibitors. *Proc. Natl. Acad. Sci. USA* **90:**8131–8135 (1993).
31. René, B., P. Fossé, T. Khélifa, A. Jacquemin-Sablin, and C. Bailly. The 1′-substituent on the anilino ring of the antitumor drug amsacrine is a critical element for topoisomerase II inhibition and cytotoxicity. *Mol. Pharmacol.* **49:**343–350 (1996).
32. Subra, F., S. Carteau, J. Pager, J. Paoletti, C. Paoletti, C. Auclair, D. Mrani, G. Gosselin, and J. L. Imbach. Bis(pyrrolecarboxamide) linked to intercalating chromophore oxazolopyridocarbazole (OPC): selective binding to DNA and polynucleotides. *Biochemistry* **30:**1642–1650 (1991).
33. Berger, J. M., S. J. Gamblin, S. C. Harrison, and J. C. Wang. Structure and mechanism of DNA topoisomerase II. *Nature (Lond.)* **379:**225–232 (1996).
34. Capranico, G., K. W. Kohn, and Y. Pommier. Local sequence requirements for DNA cleavage by mammalian topoisomerase II in the presence of doxorubicin. *Nucleic Acids Res.* **18:**6611–6619 (1990).
35. Pommier, Y., G. Capranico, A. Orr, and K. W. Kohn. Local base sequence preferences for DNA cleavage by mammalian topoisomerase II in presence of amsacrine or teniposide. *Nucleic Acids Res.* **19:**5973–5980 (1991).
36. Huff, A. C., R. G. Robinson, A. C. Evans, K. N. Selander, M. P. Wentland, J. B. Rake, and S. A. Coughlin. DNA sequence preference at sites cleaved by human DNA topoisomerase II in response to novel quinolone derivatives. *Anti-Cancer Drug Des.* **10:**251–276 (1995).
37. Howard, M. T., M. P. Lee, T. Hsieh, and J. D. Griffith. *Drosophila* topoisomerase II-DNA interactions are affected by DNA structure. *J. Mol. Biol.* **217:**53–62 (1992).
38. Udvardy, A., and P. Schedl. Chromatin structure, not DNA sequence specificity, is the primary determinant of topoisomerase II sites of action in vivo. *Mol. Cell. Biol.* **11:**4973–4984 (1991).
39. Borgnetto, M. E., F. Zunino, S. Tinelli, E. Käs, and G. Capranico. Drug-specific sites of topoisomerase II DNA cleavage in *Drosophila* chromatin: heterogeneous localization and reversibility. *Cancer Res.* **56:**1855–1862 (1996).

Send reprint requests to: Dr. Christian Bailly, Institut de Recherches sur le Cancer, INSERM Unité 124, Place de Verdun, 59045 Lille, France. E-mail: bailly@lille.inserm.fr